Available online at www.sciencedirect.com
SCIENCE DIRECT®
Bioorganic & Medicinal Chemistry Letters 15 (2005) 1101–1106
Bioorganic & Medicinal Chemistry Letters

Structure-based design of potent and selective inhibitors of collagenase-3 (MMP-13)

Soong-Hoon Kim,* Andrew T. Pudzianowski, Kenneth J. Leavitt, Joseph Barbosa, Patricia A. McDonnell, William J. Metzler, Bruce M. Rankin, Richard Liu, Wayne Vaccaro and William Pitts

Bristol Myers Squibb Co., Pharmaceutical Research Institute, PO Box 4000, Princeton, NJ 08560, USA

Received 17 September 2004; revised 1 December 2004; accepted 8 December 2004
Available online 7 January 2005

Abstract—Computer aided drug design led to a new class of spiro-barbiturates (e.g., **4a**, MMP-13 $K_i = 4.7$ nM) that are potent inhibitors of MMP-13.

The matrix metalloproteinases (MMPs) belong to a family of zinc proteases that are important in homeostasis of extra-cellular matrix proteins.[1] They have been implicated in several pathologies including cancer, osteoarthritis, and rheumatoid arthritis.[2]

Osteoarthritis is a degenerative disease characterized by the loss of joint function and articular cartilage. Current therapies, such as COX-2 inhibitors and non-steroidal anti-inflammatory agents, target signs, and symptoms. Disease modifying osteoarthritis drugs that may delay disease progression are not presently available.

Although the inhibition of MMP-13 as a treatment for osteoarthritis has not been clinically validated, pre-clinical data suggest MMP-13 as a compelling target for the modulation of osteoarthritis. Articular cartilage consists of type II collagen and proteoglycan, and studies have shown that MMP-13 (collagenase-3) cleaves type II collagen.[3] MMP-13 over-expression induces osteoarthritis in transgenic mice, and MMP-13 mRNA expression is co-distributed with the type II collagenase activity in osteoarthritis cartilage.[4] Thus, the data strongly suggest that inhibition of MMP-13 may lead to inhibition of cartilage degradation associated with osteoarthritis. A major effort is in progress by several research groups to discover selective small molecule inhibitors of MMP-13.[5]

Historically, most MMP inhibitors have been based on hydroxamic acids.[6] In general, hydroxamic acid based inhibitors are remarkably potent (e.g., RS-130830 **1**, MMP-13 $K_i = 0.52$ nM, Fig. 1).[7] Nevertheless, a growing body of evidence suggests that hydroxamic acids have poor pharmacokinetic profiles, exemplified by poor absorption and rapid metabolism.[8] Despite these potential shortcomings several hydroxamic acid based MMP inhibitors have been in human clinical trials.[9] Because of these potential liabilities, our goal was to design a

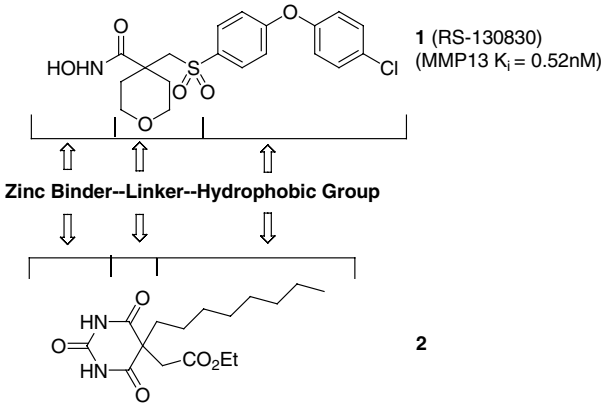

Figure 1. Functional mapping of MMP inhibitors.

Keywords: MMP-13 inhibition; Barbituric acid; Structure-based design.
* Corresponding author. Tel.: +1 609 252 4079; fax: +1 609 252 3993; e-mail: soonghoon.kim@bms.com

0960-894X/$ - see front matter © 2004 Elsevier Ltd. All rights reserved.
doi:10.1016/j.bmcl.2004.12.016

series of potent MMP-13 inhibitors which did not contain a hydroxamic acid. An additional goal was to identify an inhibitor of MMP-13 with a good degree of selectivity among MMP and ADAM family members (e.g., MMP-1, MMP-2, MMP-12, and TACE).

MMP inhibitors have been widely studied and extensively reviewed.[5,6] Most potent MMP inhibitors share two common structural features: a Lewis base that interacts with the catalytic Zn(II); and a hydrophobic group that is in contact with the binding pocket (Fig. 1). Among the zinc chelators, hydroxamic acids have been used extensively to produce potent enzyme inhibition. Barbituric acid based inhibitors, as exemplified by inhibitor **2**, appear to provide an interesting alternative to hydroxamic acid based inhibitors. Though its potency against MMP-13 has not been reported, compound **2** is reported to be an inhibitor of MMP-8 (IC_{50} = 107 nM), and MMP-9 (IC_{50} = 20 nM).[5,10] Since the appearance of **2** in the literature, there have been reports from other laboratories reporting successful incorporation of barbituric acids into inhibitors of MMPs, including MMP-13.[10c] Thus the use of a barbiturate as a zinc ligand seemed to be a reasonable starting point for the design of a potent and selective inhibitor of MMP-13.

Barbituric acid could in principle bind to a zinc atom via interactions with either a carbonyl oxygen, a ring nitrogen or a combination of the two atoms.[11] To aid inhibitor design, we first sought to gain a better understanding of how a barbituric acid might be bound to zinc in the active site of an MMP by building a model system.[12] Semiempirical AM1[13] calculations with *tert*-butyl hydroxamate (HONHCO-*tert*-butyl) and tris-imidazole Zn(II), reproduced the bidentate mode of interaction with slightly longer (calculated: 2.13 Å and 2.34 Å; the complexation enthalpy, relative to separated *tert*-butyl hydroxamate and tris-imidazole Zn(II) is $\Delta H_{cx} = -108.3$ kcal/mol) zinc–oxygen bond distances when compared to those found in RS-130830/MMP-13 crystal structure (X-ray structure bond lengths: 1.9 Å and 2.1 Å).[14] The longer bond length is characteristic of AM1 calculations. AM1 optimization with a barbituric acid **3** showed that a monodentate nitrogen–Zn(II) interaction was the most enthalpically favored, with a Zn(II)–nitrogen distance of 2.09 Å (enthalpy of complexation: $\Delta H_{cx} = -91.8$ kcal/mol). An overlay of *tert*-butyl hydroxamate and barbituric acid **3** is shown in Figure 2.[15]

Based on our understanding of the barbiturate–zinc interaction and the reported X-ray structure of RS-130830 **1** bound to MMP-13 we sought to apply structure-based design to produce potent barbiturate containing inhibitors of this enzyme (see Fig. 3). The X-ray structure of RS-130830 provides the distance from hydroxamate to zinc ion and the relative distance from the hydroxamate to the biaryl ether group. The barbiturate zinc model system described above was utilized to suggest a reasonable starting conformation for projection into the binding pocket from the barbiturate ligand. Finally, a linker structure that retained the bound conformation of RS-130830 was designed to provide both constraint and a novel structural motif. The linker region of RS-130830 that joins the hydroxamic acid to the biaryl ether group contains at least two bonds that are to some extent freely rotating and it is unknown if

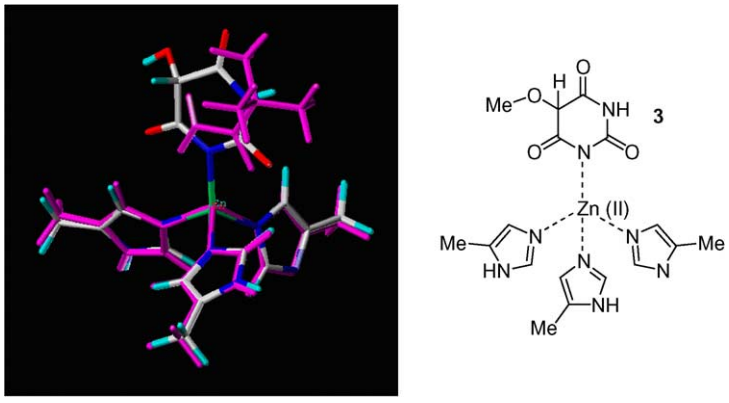

Figure 2. Structure of Zn(II) tris-imidazole with barbituric acid **3** (gray) and its overlay with *tert*-butyl hydroxamate (magenta). Note that complex is electrically neutral.

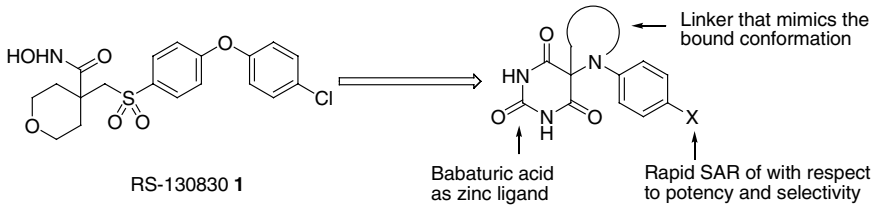

Figure 3. Design features for a selective, non-hydroxamate acid inhibitor of MMP-13.

the compound shows significant conformational preference in solution. In principle, a linker structure that mimics the bound conformation of acyclic **1** should be entropically favored (pre-organization).[16]

Several constrained linkers fit both the conformational profile of the docked inhibitor **1** to MMP-13 and the calculated constraint of the barbituric acid–zinc interaction. Specifically, modeling predicts that the ground state conformation of spiro-barbiturate **4a** to be nearly identical with the bound conformation of inhibitor **1** in the MMP-13 active site.[17] An overlay of spiro-barbiturate **4a** with RS-130830 **1** is shown in Figure 4. It is interesting to note that the carbonyl oxygen in the

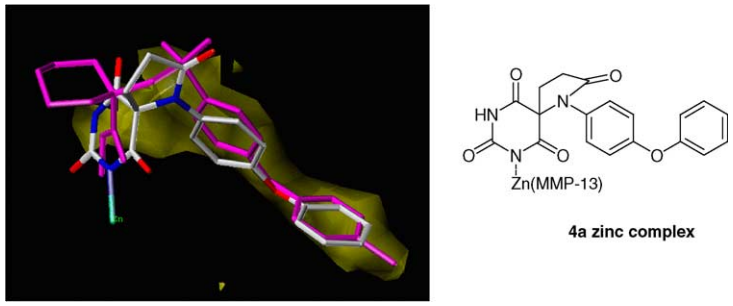

Figure 4. Modeled structure of barbituric acid **4a** in MMP-13 and its overlap with the bound structure of RS-130830 **1** (magenta). Also shown is the MOL2MAP methyl probe interaction energy contour at −1.8 kcal/mol (yellow) for the RS-130830 binding site.

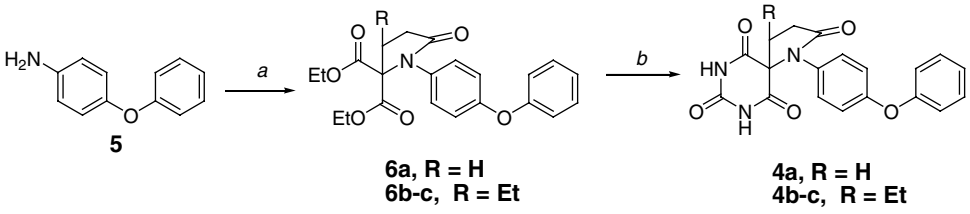

Scheme 1. Reagents and conditions: (a) diethylbromomalonate, toluene, 100 °C, 36 h (45%); ethylacrylate (**6a**) or methyl *trans*-2-pentenoate (**6b** and **c**), NaOEt/EtOH, 80 °C, 3 h (69–71%); (b) urea, NaOEt, EtOH, 80 °C, 5 h (36–44%).

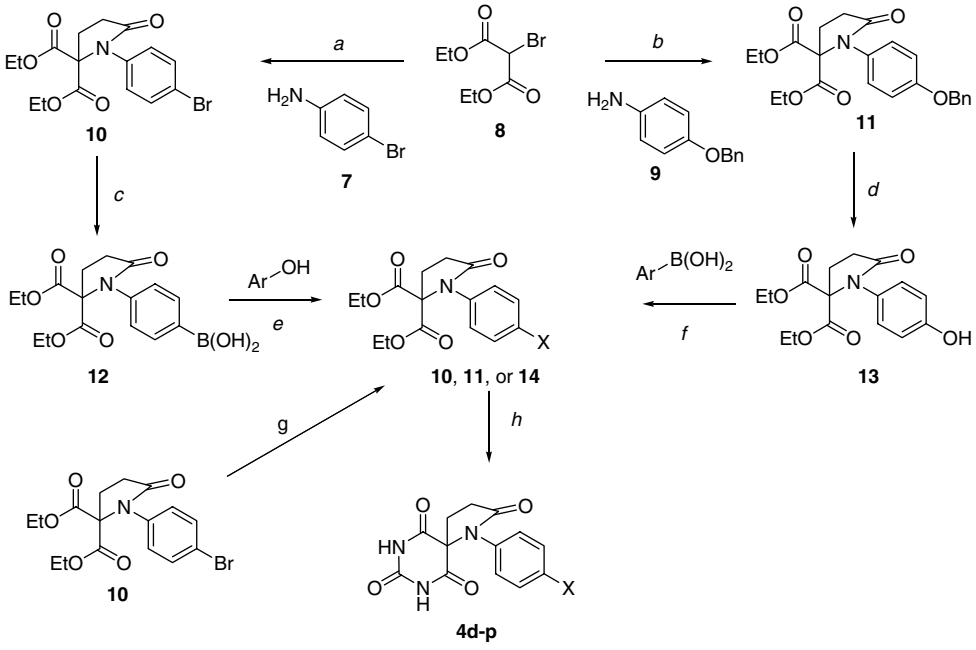

Scheme 2. Reagents and conditions: (a) **7**, DMF, 100 °C, ethyl acrylate, NaOEt, EtOH, 3 h (41%); (b) **9**, DMF, 100 °C, ethyl acrylate, NaOEt, EtOH, 3 h (45%); (c) Pd(dppf), bis(pinacolato)diboron, KOAc, DMSO, 65 °C, 3 h; $NaIO_4$, NH_4OAc, acetone/H_2O (1:1), rt, 3 h (82%); (d) H_2 (balloon), 10% Pd–C, 1 h, DMF (92%); (e) ArOH, $Cu(OAc)_2$, TEA, CH_2Cl_2, rt, 12 h (57–62%); (f) $ArB(OH)_2$, $Cu(OAc)_2$, TEA, CH_2Cl_2, rt, 12 h (79–85%); (g) for X = H: H_2 (balloon), 10% Pd–C, EtOH, rt, 5 h (86%); for X = Ph: $PhB(OH)_2$, $Pd(dppf)Cl_2$, K_3PO_4, 65 °C, 3.5 h (93%); (h) urea, NaOEt, EtOH, 80 °C (35–55%).

Table 1. SAR of aromatic substitution

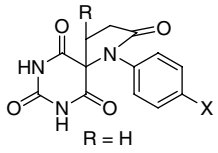

Compd	X	MMP-13 K_i (nM)[a]
4d	H	2200
4e	Br	130
4a	OPh	4.7
4f	Ph	934
4g	OBn	1100
4h	OPh(4-Cl)	0.95
4i	OPh(3-Cl)	54
4j	OPh(3-OMe)	1.9
4k	OPh(2-OMe)	110
4l	OPh-3,4-(OCH_2O)	5.8
4m	O(4-OMe-3-pyridyl)	25
4n	OPh(4-CO_2Me)	4.2
4o	OPh(4-CO_2H)	2.7
4p	OPh(4-OPh)	0.33

[a] With the exception of compounds **4d**, **4e**, and **4g** (single runs, MMP-13 IC_{50}), all compounds in Tables 1 and 2 are reported as K_is and based on triplicate runs with standard deviation of less than 15%.[20]

lactam ring of **4a** overlaps well with one of the sulfone oxygen atoms in inhibitor **1**.

The synthesis of compounds **4a**–**c** is shown in Scheme 1. Alkylation of 4-phenoxyaniline **5** with bromodiethylmalonate followed by condensation with either ethyl acrylate or methyl *trans*-2-pentenoate provided **6a**–**c**. Condensation of **6a**–**c** with urea provided the desired spiro-barbiturates **4a**–**c**.[18]

Once it was determined that **4a** was a potent inhibitor of MMP-13, a flexible synthetic route which permitted late stage diversification of the terminal aryl group was designed as shown in Scheme 2. Boronic acid and $Cu(OAc)_2$ mediated oxidative couplings were chosen as a means of accessing a wide range of substitution.[19] Condensation of malonates **10**, **11**, or **14** with urea provided inhibitors **4d**–**p**.

Spiro-barbiturate **4h** is a potent inhibitor of MMP-13 (K_i = 0.95 nm). Its potency suggests that it interacts with MMP-13 in a manner similar to RS-130830 and validates the structure based de novo design of an MMP-13 inhibitor. Examination of the SAR (Table 1) shows that MMP-13 potency is maintained with a variety of aryloxy systems. Replacement of the aryloxy group by hydrogen (**4d**) results in nearly a 500-fold loss in potency. It is interesting to note that the biphenyl analogue **4f** (K_i = 934 nm) is significantly less potent against MMP-13 than compound **4a**. In general *para*-substitution on the aryl ring provided the most potent analogs (**4h**,**m**,**n**,**o**,**p**).

MMPs are structurally similar but show differences in the S1′ binding pocket, thus the region of inhibitor (P1′) that interacts with S1′ is likely to be important to selectivity. Deep S1′ binding pockets are found in MMP-13, MMP-12, MMP-9, MMP-3, MMP-2, and TACE; shallow S1′ pockets are found in MMP-1 and MMP-7.[21] In general the compounds in Table 2 have a improved selectivity for MMP-13 compared to that reported for RS-130830 **1**;[7] however, there was no significant difference among the compounds with respect to selectivity against MMP-2 and MMP-9. The data for enantiomers **4b** and **4c** suggest that chirality in the linker region had an effect on MMP-13 potency but no major effect on the selectivity profile.

Pre-clinical evidence suggests that inhibition of MMP-13 could be useful in osteoarthritis and rheumatoid arthritis. The spiro-barbiturates **4b** and **4p** have a similar potency and improved MMP-3 selectivity compared to the hydroxamic acid based inhibitor **1**, (RS-130830). MMP-13 structural information, together with AM1 calculation of the Zn(II)–barbiturate interaction, led to a predictive binding model which played a crucial role in the selection process of the initial constrained lead **4a**.[15,22] Although significant selectivity against the MMP-2 and MMP-9 was not achieved for the compounds reported, this work demonstrates that appropriately substituted barbituric acids can achieve similar potency to hydroxamic acid based systems.

Table 2. Selectivity SAR of compounds **4a**–**p**

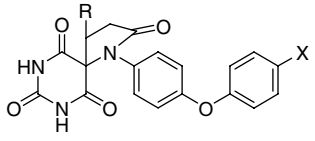

Compd	R	X	MMP-1 K_i (nM)	MMP-2 K_i (nM)	MMP-3 K_i (nM)	MMP-9 K_i (nM)	MMP-13 K_i (nM)	TACE K_i (nM)
1[a]	—	—	590	0.22	9.3	0.55	0.52	—
4a	H	H	>5000	1.6	4500	4.7	4.7	>1000
4b	Et	H	>5000	0.40	92	0.87	0.54	>1000
4c	Et	H	>5000	1.7	1200	7.2	4.1	>1000
4h	H	Cl	>5000	0.43	430	0.72	0.95	>1000
4n	H	CO_2Me	>5000	4.7	1300	1.2	4.2	>1000
4o	H	CO_2H	>5000	0.23	3200	0.72	2.7	>1000
4p	H	OPh	>5000	1.8	110	1.9	0.33	>1000

[a] Data for compound **1** reported Ref. 7.

References and notes

1. (a) Johnson, L. L.; Dyer, R.; Hupe, D. J. *Curr. Opin. Chem. Biol.* **1998**, *2*, 466; (b) Shapiro, S. D. *Curr. Opin. Chem. Biol.* **1998**, *10*, 602; (c) Whittaker, M.; Floyd, C. D.; Brown, P.; Gearing, J. H. *Chem. Rev.* **1999**, *9*, 2735; (d) Nagase, H.; Woessner, J. F., Jr. *J. Biol. Chem.* **1999**, *274*, 21491.
2. (a) Firestein, G. S.; Paine, M. M.; Littman, B. H. *Arthritis Rheum.* **1992**, *34*, 1094; (b) Walakovits, L. A.; Bhardwaj, N.; Gallick, G. S.; Lark, M. W.; Clark, I. M. *Arthritis Rheum.* **1992**, *35*, 35; (c) Clark, I. M.; Rowan, A. D.; Cawston, T. E. *Curr. Opin. Anti-Inflam. Immunomod. Invest. Drugs* **2000**, *2*, 16; (d) Bottomley, K. M.; Johnson, W. H.; Walter, D. S. *J. Enzyme Inhib.* **1998**, *13*, 79; (e) Yip, D.; Ahmad, A.; Karapetis, C. S.; Hawkins, C. A.; Harper, P. G. *Invest. New Drugs* **1999**, *17*, 387.
3. Freemont, A. J.; Byers, R. J.; Taiwo, Y. O.; Hoyland, J. A. *Ann. Rheum. Dis.* **1999**, *58*, 357.
4. (a) Neuhold, L. A.; Killar, L.; Zhao, W.; Sung, M.; Warner, L.; Kulik, J.; Turner, J.; Wu, W.; Billinghurst, C.; Meijers, T.; Poole, A. R.; Babij, P.; DeGennaro, L. J. *J. Clin. Invest.* **2001**, *1*, 35; (b) Konttinen, Y. T.; Ainola, M.; Valleala, H.; Ma, J.; Ida, H.; Mandelin, J.; Kinne, R. W.; Santavirta, S.; Sorsa, T.; Lopez-Otin, C.; Takagi, M. *Ann. Rheum. Dis.* **1999**, *58*, 691.
5. For an excellent review on the design and application of matrix metalloproteinase inhibitors see Skiles, J. W.; Gonnella, N. C.; Jeng, A. Y. *Curr. Med. Chem.* **2001**, *8*, 425.
6. (a) Skotnicki, J. S.; Levin, J. I.; Zask, A.; Killar, L. M. In *Metalloproteinases as Targets for Anti-Inflammatory Drugs*; Bottomley, K. M. K., Bradshaw, D., Nixon, J. S., Eds.; Birkhauser: Basel, 1999; pp 17–57; (b) Clark, I.; Parker, A. E. *Exp. Opin. Ther. Targets* **2003**, *7*, 19.
7. Campbell, J. A. *Book of Abstracts*, 216th ACS National Meeting of the American Chemical Society, 1998.
8. (a) Bender, S. Lecture at the Second Winter Conference on Medicinal Chemistry, Steamboat Springs, CO, Jan 26–31, 1997; (b) Tamura, Y.; Watanabe, F.; Nakatani, T.; Yasui, K.; Fuji, M.; Komurasaki, T.; Tsuzuki, H.; Maekawa, R.; Yoshioka, T.; Kawada, K.; Sugita, K.; Ohtani, M. *J. Med. Chem.* **1998**, *41*, 1749; (c) Whittaker, M.; Floyd, C. D.; Brown, P.; Gearing, A. J. *Chem. Rev.* **1999**, *99*, 2735.
9. Shaw, T.; Nixon, J. S.; Bottomley, K. M. *Exp. Opin. Invest. Drugs* **2000**, *9*, 1469–1478.
10. Barbituric acids: (a) Oliva, A.; De Cellis, G.; Grams, F.; Livi, V.; Zimmermann, G.; Menta, E.; Krell, H. -W., PCT Int. Appl. WO 9858925, Dec 30, 1998; (b) Grams, F.; Mermann, G. PCT Int. Appl. WO 9858915, Dec 30, 1998; (c) Foley, L. H.; Palermo, R.; Dunten, P.; Wang, P. *Bioorg. Med. Chem. Lett.* **2001**, *11*, 969; (d) Brandstetter, H.; Grams, F.; Glitz, D.; Lang, A.; Huber, R.; Bode, W.; Krell, H.; Engh, R. A. *J. Biol. Chem.* **2001**, *20*, 17405; (e) Dunten, P.; Kammloft, U.; Crother, W. L.; Foley, L. H.; Wang, P.; Palermo, R. *Protein Sci.* **2001**, *10*, 923; (f) Other heterocycles: Puerta, T. D.; Lewis, J. A.; Cohen, S. M. *J. Am. Chem. Soc.* **2004**, *126*, 8388; (g) Jacobsen, E. J.; Mitchell, M. A.; Hendges, S. K.; Belonga, K. L.; Skaletzky, L. L.; Stelzer, L. S.; Lindberg, T. J.; Fritzen, E. L.; Schostarez, H. J.; O'Sullivan, T. J.; Maggiora, L. L.; Stuchly, C. W.; Laborde, A. L.; Kubicek, M. F.; Poorman, R. A.; Beck, J. M.; Miller, H. R.; Petzold, G. L.; Scott, P. S.; Truesdell, S. E.; Wallace, T. L.; Wilks, J. W.; Fisher, C.; Goodman, L. V.; Kaytes, P. S.; Ledbtter, S. R.; Powers, E. A.; Vogeli, G.; Mott, J. e.; Trepod, C. M.; Staples, D. J.; Baldwin, E. T.; Finzel, B. C. *J. Med. Chem.* **1999**, *42*, 1525.
11. Wang, B. C.; Craven, B. M. *J. Chem. Soc., Chem. Commun.* **1971**, *7*, 290. An X-ray structure of a barbituric acid–Zn(II) inorganic complex.
12. The calculations of zinc–barbituric (BA) interaction, target synthesis, and in vitro evaluation were carried out prior to the public disclosure of X-ray crystal structures of barbituric acid bound to MMPs (Ref. 10d and e).
13. **AM1**: Dewar, M. J. S.; Zoebisch, E. G.; Healy, E. F.; Stewart, J. P. *J. Am. Chem. Soc.* **1985**, *107*, 3902.
14. Lovejoy, B.; Welch, A. R.; Carr, S.; Luong, C.; Broka, C.; Hendricks, T.; Campbell, J. A.; Walker, K. A. M.; Martin, R.; Wart, H. V.; Browner, M. F. *Nat. Struct. Biol.* **1999**, *6*, 217.
15. The overlap of calculated structure in Figure 2 versus reported barbiturate MMP inhibitor structures is very good. The calculated zinc–nitrogen distance is 2.09 Å, which is in line with the distances of 2.09 Å and 2.17 Å found for zinc–nitrogen bond (Ref. 10d and e, respectively). The reported zinc–oxygen distances of 2.9 Å (MMP-8, Ref. 10d) and 3.0 Å (Stromelysin, Ref. 10e) are significantly longer than the zinc–oxygen distance of 1.9 Å found in a hydroxamate/MMP structure.[14] Interestingly an inorganic-complex containing of Zn(II) and barbituric acid shows little evidence that it forms a bidentate chelate.[11] Thus it may not be necessary to invoke a bidentate binding mode for the barbituric acid–zinc interaction (penta-coordination around zinc). Importantly, there is a good agreement between the X-ray and calculated structures which suggests that calculations may play an important role in the design of new non-hydroxamic acid based inhibitors of MMPs (see for instance, Ref. 10e). Another consideration is the ionization state of the barbituric acid. The calculation was carried out using deprotonated barbituric acid, with the ligand bearing a formal −1 charge. Calculations could not produce a stable complex when the neutral barbiturate forms were substituted (data not shown.) The pK_a for **4a** was experimentally determined to be 6.4(±0.2) (spectrophotometric titration in water). Thus, the possibility that the ionized specie is the catalytically active form cannot be ruled out, however both Ref. 10d and e suggest the barbituric acid is bound to MMPs in a neutral form.
16. Cram, D. J.; Trueblood, K. N. In *Host Guest Complex Chemistry*; Vogtle, E., Weber, E., Eds.; Springer: Berlin, 1985; pp 1–42.
17. (a) The available X-ray coordinates of **1** with MMP-13[14] were used in the SYBYL program to arrive at binding site descriptors, including MOL2MAP surface grids that provide chemical probe interaction energy contours of the binding site. As shown in Figure 3, a tris-imidazole complex was used with the AM1 semiempirical SCF-MO methodology to examine zinc–barbiturate interaction. The calculated Zn–N barbiturate distance (2.09 Å) and geometric constraints (monodentate nitrogen chelation, tetrahedral L–Zn–L of 109.5°) were built into the Tripos molecular mechanics force field (Tripos FF). Inhibitor modeling was initiated with a SAM1 optimized structure of the inhibitor, for example, **4a**, inserted into the MMP-13 binding site. The entire protein/inhibitor aggregate was then allowed to relax for 1000 iterations of geometry optimization with the Tripos force field, resulting in the structure shown in Figure 4; (b) SYBYL: Tripos, Inc., 1699 S. Hanley Road, St. Louis MO 63144-2913(c) MOL2MAP: MOL2MAP is a FORTRAN program with SYBYL SPL interface (A. T. Pudzianowski) based on the original GRID methodology:

Goodford, P. J. *J. Med. Chem.* **1985**, *28*, 849; (d) **Tripos FF:** Clark, M.; Cramer, R. D., III; Van Opdenbosch, N. *J. Comp. Chem.* **1989**, *10*, 982; (e) **SAM1**: Dewar, M. J. S.; Jie, C.; Yu, G. *Tetrahedron* **1993**, *23*, 5003, SAM1 is implemented in AMPAC 6.0, Semichem, Inc., 7204 S. Mullen, Shawnee KS 66216 (1997).

18. Enantiomers **4b** and **4c** were separated by preparatory chiral HPLC using a Chiracel AS column, isocratic gradient 40% (1:1 MeOH/EtOH) 60% hexane, **4b** (R_t = 15 min), **4c** (R_t = 18.5 min).
19. Lam, P. Y. S.; Clark, C. G.; Saubern, S.; Adams, J.; Averill, K. M.; Chan, D. M. T.; Combs, A. *Synlett* **2000**, 674.
20. Copeland, R. A.; Lombardo, D.; Giannaras, J.; Decicco, C. P. *Bioorg. Med. Chem. Lett.* **1995**, *5*, 1947.
21. Borkakoti, N. In *Metalloproteinases as Targets for Anti-Inflammatory Drugs*; Bottomley, K. M. K., Bradshaw, D., Nixon, J. S., Eds.; Birkhauser: Basel, 1999; pp 17–57.
22. Structural characterization of **4a** bound to MMP-13 will be reported in due course.